

ARTICLES

Excitation energies for a benchmark set of molecules obtained within time-dependent current-density functional theory using the Vignale–Kohn functional

M. van Faassen and P. L. de Boeij

Theoretical Chemistry, Materials Science Centre, Rijksuniversiteit Groningen, Nijenborgh 4, 9747 AG Groningen, The Netherlands

(Received 19 January 2004; accepted 18 February 2004)

In this article we explain how the existing linear response theory of time-dependent density-functional theory can be extended to obtain excitation energies in the framework of time-dependent current-density-functional theory. We use the Vignale–Kohn current-functional [G. Vignale and W. Kohn, *Phys. Rev. Lett.* **77**, 2037 (1996)] which has proven to be successful for describing ultranonlocal exchange-correlation effects in the case of the axial polarizability of molecular chains [M. van Faassen, P. L. de Boeij, R. van Leeuwen, J. A. Berger, and J. G. Snijders, *Phys. Rev. Lett.* **88**, 186401 (2002); *J. Chem. Phys.* **118**, 1044 (2003)]. We study a variety of singlet excitations for a benchmark set of molecules. The $\pi^* \leftarrow \pi$ transitions obtained with the Vignale–Kohn functional are in good agreement with experiment and other theoretical results and they are in general an improvement upon the adiabatic local density approximation. In case of the $\pi^* \leftarrow n$ transitions the Vignale–Kohn functional fails, giving results that strongly overestimate the experimental and other theoretical results. The benchmark set also contains some other types of excitations for which no clear failures or improvements are observed. © 2004 American Institute of Physics. [DOI: 10.1063/1.1697372]

I. INTRODUCTION

Time-dependent density-functional theory has the potential to be a very versatile method to calculate excitation and response properties of large molecular systems. The theory is in principle exact and for many systems even simple approximations for the exchange-correlation potential yield a method that becomes competitive in accuracy with other advanced many-particle approaches.^{1–3} However, in some cases simple approximations like the standard adiabatic local density approximation (ALDA) do not suffice.

An important example is the static axial polarizability of conjugated oligomers, which is greatly overestimated within the ALDA. This local approximation and also more advanced generalized gradient approximations are unable to describe the highly nonlocal exchange and correlation effects found in these quasi-one-dimensional systems.^{4,5} One route to overcome these shortcomings is to employ optimized effective potentials⁶ derived from the energy functional that includes exact exchange (see Refs. 7 and 8, and references therein), or approximations to this potential such as the Krieger–Li–Iafrate⁹ and common-energy-denominator approximations.^{10,11}

In our previous works, Refs. 12 and 13, we have found a successful alternative approach towards the solution of this longstanding problem by using time-dependent current-density-functional theory, in which we describe ultranonlocal exchange-correlation effects within a local current description. For this we used the Vignale–Kohn (VK) current-

functional. They were the first to propose such a functional^{14,15} in which the current-density is used as a local indicator of global changes. From a careful analysis of the weakly inhomogeneous perturbed electron gas they arrived at an expression^{14–17} for the first-order induced exchange-correlation contributions in the form of a viscoelastic stress field.

For the prototype polyacetylene and many other systems the results obtained significantly improved upon the ALDA results and were in excellent agreement with high level *ab initio* quantum chemical methods. However, we also observed that a similar large correction was not obtained for a hydrogen chain having alternating bond lengths that is seen as a theoretical model for conjugated systems (see Ref. 18, and references therein). This indicates that the VK functional is not able to describe all features necessary for a correct description of the axial polarizability.

To test the VK functional further, we calculated excitation energies for a collection of molecules and analyze the way in which the VK-functional modifies the ALDA results for the excitation properties. This benchmark set mainly consists of the collection of molecular excitations devised by Parac and Grimme¹⁹ to benchmark their multireference second-order Møller–Plesset (MR-MP2) method. They chose their set such that accurate experimental data are available and that a broad range of chemical structures with states of nontrivial electronic character is covered. For our purpose we added three other excitations to this set: the prototype $\pi^* \leftarrow \pi$ excitation in ethylene and the prototype $\pi^* \leftarrow n$ ex-

citation in formaldehyde, and finally as example of an excitation in a molecular chain the $1^1B_u \pi^* \leftarrow \pi$ excitation in *trans*-1,3,5,7,9-decapentaene.

In this article we will describe the theory needed to obtain excitation energies within the time-dependent current-density-functional approach and we will present and discuss our results for the benchmark set of molecules. In a future article we will study the excitation energies for the long molecular chains as a function of chain length.

II. THEORY

A. Excitation energies within time-dependent current-density-functional theory

The theory behind the calculation of excitation energies within the TD-DFT is extensively studied. Good descriptions of this theory can be found in Refs. 2, 20, 21. To use a functional that is dependent on the current-density, such as the Vignale–Kohn (VK) functional, one needs to extend this theory to time-dependent current-density-functional theory (TD-CDFT). Because much of the derivations are analogues to the ordinary TD-DFT case we will focus here on the differences needed to include the current density.

We will consider the response of systems with a ground state that is described within a spin-restricted formulation. However, we consider the response for each spin component separately. The time-dependent Kohn–Sham equations within the TD-CDFT are

$$\begin{aligned} & \left\{ \frac{1}{2} (-i\nabla + \mathbf{A}_{\text{eff},\sigma}(\mathbf{r},t))^2 + v_{\text{eff},\sigma}(\mathbf{r},t) \right\} \phi_{n\sigma}(\mathbf{r},t) \\ &= i \frac{\partial}{\partial t} \phi_{n\sigma}(\mathbf{r},t), \end{aligned} \quad (1)$$

where σ indicates the spin component. The time-dependent effective potentials $v_{\text{eff},\sigma}(\mathbf{r},t)$ and $\mathbf{A}_{\text{eff},\sigma}(\mathbf{r},t)$ are uniquely determined by the exact time-dependent density and current density. These densities can be obtained from the orbitals $\phi_{n\sigma}(\mathbf{r},t)$ by

$$\rho_{\sigma}(\mathbf{r},t) = \sum_n f_{n\sigma} \phi_{n\sigma}^*(\mathbf{r},t) \phi_{n\sigma}(\mathbf{r},t) \quad (2)$$

and

$$\begin{aligned} \mathbf{j}_{\sigma}(\mathbf{r},t) &= \sum_n f_{n\sigma} \frac{-i}{2} [\phi_{n\sigma}^*(\mathbf{r},t) \nabla \phi_{n\sigma}(\mathbf{r},t) \\ &\quad - \phi_{n\sigma}(\mathbf{r},t) \nabla \phi_{n\sigma}^*(\mathbf{r},t)] + \rho_{\sigma}(\mathbf{r},t) \mathbf{A}_{\text{eff},\sigma}(\mathbf{r},t). \end{aligned} \quad (3)$$

Here $f_{n\sigma}$ are the occupation numbers, where for the spin-restricted case $f_{n\uparrow} = f_{n\downarrow} = 1$ for the occupied states and $f_{n\uparrow} = f_{n\downarrow} = 0$ for the unoccupied states. We assume that there are no fractional occupation numbers. Equation (3) denotes the physical current density, that is, the sum of the diamagnetic and paramagnetic contributions. This physical current density is gauge invariant. For purely longitudinal vector potentials (which can be gauge transformed into scalar potentials), the density calculated from Eq. (2) is identical to that calculated from the time-dependent Kohn–Sham equations of pure density functional theory.

To obtain the excitation energies we will use linear response theory. Within the regime of linear response the first order changes in the scalar and vector potential are given by,

$$\delta v_{\text{eff},\sigma}(\mathbf{r},\omega) = \delta v_H(\mathbf{r},\omega) + \delta v_{\text{xc},\sigma}(\mathbf{r},\omega) \quad (4)$$

and

$$\delta \mathbf{A}_{\text{eff},\sigma}(\mathbf{r},\omega) = \delta \mathbf{A}_{\text{ext}}(\mathbf{r},\omega) + \delta \mathbf{A}_{\text{xc},\sigma}(\mathbf{r},\omega), \quad (5)$$

where $\delta v_H(\mathbf{r},\omega)$ represents the first order change in the Hartree potential, $\delta \mathbf{A}_{\text{ext}}(\mathbf{r},\omega)$ is the external field, and $\delta v_{\text{xc},\sigma}(\mathbf{r},\omega)$ and $\delta \mathbf{A}_{\text{xc},\sigma}(\mathbf{r},\omega)$ are the first order changes in the spin dependent scalar and vector xc-potentials. Note that the external field is completely represented by the vector potential $\delta \mathbf{A}_{\text{ext}}(\mathbf{r},\omega)$, i.e., $\delta v_{\text{ext}}(\mathbf{r},\omega) = 0$, and that we use the Coulomb gauge for the induced potentials. For this gauge choice $\delta \mathbf{A}_{\text{ind}}(\mathbf{r},\omega) = 0$ if we neglect retardations²² and microscopic magnetic effects. This is consistent with the neglect of the Breit^{23,24} corrections in the ground-state calculation. In this particular formulation we choose the gauge for the xc-contribution such that only terms linear in $\delta \rho_{\uparrow}(\mathbf{r},\omega)$ and $\delta \rho_{\downarrow}(\mathbf{r},\omega)$ are retained in $\delta v_{\text{xc},\sigma}(\mathbf{r},\omega)$, while all terms linear in $\delta \mathbf{j}_{\uparrow}(\mathbf{r},\omega)$ and $\delta \mathbf{j}_{\downarrow}(\mathbf{r},\omega)$ are gauge transformed to $\delta \mathbf{A}_{\text{xc},\sigma}(\mathbf{r},\omega)$. In this way we keep contact with the ordinary TDDFT formulation. Due to the continuity equation $\nabla \cdot \delta \mathbf{j}_{\sigma}(\mathbf{r},\omega) - i\omega \delta \rho_{\sigma}(\mathbf{r},\omega) = 0$, which holds for each spin component separately, we can consider $\delta \rho_{\sigma}(\mathbf{r},\omega)$ as a functional of $\delta \mathbf{j}_{\sigma}(\mathbf{r},\omega)$. Therefore $\delta \mathbf{A}_{\text{xc},\sigma}[\delta \mathbf{j}_{\uparrow}, \delta \mathbf{j}_{\downarrow}]$ is a functional of $\delta \mathbf{j}_{\uparrow}(\mathbf{r},\omega)$ and $\delta \mathbf{j}_{\downarrow}(\mathbf{r},\omega)$ only. The first order changes in the xc-contribution can be given in the form,

$$\delta v_{\text{xc},\sigma}(\mathbf{r},\omega) = \sum_{\sigma'} \int f_{\text{xc}}^{\sigma\sigma'}(\mathbf{r},\mathbf{r}',\omega) \delta \rho_{\sigma'}(\mathbf{r}',\omega) d\mathbf{r}' \quad (6)$$

and

$$\delta \mathbf{A}_{\text{xc},\sigma}(\mathbf{r},\omega) = \sum_{\sigma'} \int \mathbf{f}_{\text{xc}}^{\sigma\sigma'}(\mathbf{r},\mathbf{r}',\omega) \delta \mathbf{j}_{\sigma'}(\mathbf{r}',\omega) d\mathbf{r}', \quad (7)$$

where $f_{\text{xc}}^{\sigma\sigma'}$ and $\mathbf{f}_{\text{xc}}^{\sigma\sigma'}$ are the spin-dependent scalar and tensor xc-kernels. For the spin restricted ground state, $f_{\text{xc}}^{\uparrow\uparrow} = f_{\text{xc}}^{\downarrow\downarrow}$, $f_{\text{xc}}^{\uparrow\downarrow} = f_{\text{xc}}^{\downarrow\uparrow}$, $\mathbf{f}_{\text{xc}}^{\uparrow\uparrow} = \mathbf{f}_{\text{xc}}^{\downarrow\downarrow}$, and $\mathbf{f}_{\text{xc}}^{\uparrow\downarrow} = \mathbf{f}_{\text{xc}}^{\downarrow\uparrow}$.

The induced density and current density are given in linear approximation by

$$\begin{aligned} \delta \rho_{\sigma}(\mathbf{r},\omega) &= \sum_{\sigma'} \int (\chi_{\rho\sigma}^{\sigma\sigma'}(\mathbf{r},\mathbf{r}',\omega) \cdot \delta \mathbf{A}_{\text{eff},\sigma'}(\mathbf{r}',\omega) \\ &\quad + \chi_{\rho\rho}^{\sigma\sigma'}(\mathbf{r},\mathbf{r}',\omega) \delta v_{\text{eff},\sigma'}(\mathbf{r}',\omega)) d\mathbf{r}' \end{aligned} \quad (8)$$

and

$$\begin{aligned} \delta \mathbf{j}_{\sigma}(\mathbf{r},\omega) &= \sum_{\sigma'} \int (\{ \chi_{\mathbf{j}\mathbf{j}}^{\sigma\sigma'}(\mathbf{r},\mathbf{r}',\omega) - \chi_{\mathbf{j}\mathbf{j}}^{\sigma\sigma'}(\mathbf{r},\mathbf{r}',0) \} \\ &\quad \cdot \delta \mathbf{A}_{\text{eff},\sigma'}(\mathbf{r}',\omega) + \chi_{\mathbf{j}\rho}^{\sigma\sigma'}(\mathbf{r},\mathbf{r}',\omega) \\ &\quad \times \delta v_{\text{eff},\sigma'}(\mathbf{r}',\omega)) d\mathbf{r}'. \end{aligned} \quad (9)$$

Equation (9) is the physical induced current density, which contains the paramagnetic and diamagnetic terms. The diamagnetic term is included using the conductivity sum rule,

$$[\chi_{\mathbf{j}\mathbf{j}}^{s,\sigma\sigma'}(\mathbf{r},\mathbf{r}',0)]_{ij} + \rho_{0,\sigma}(\mathbf{r}) \delta_{\sigma\sigma'} \delta_{ij} \delta(\mathbf{r}-\mathbf{r}') = 0, \quad (10)$$

where $\rho_{0,\sigma}(\mathbf{r})$ is the ground state density for which $\rho_{0,\uparrow}(\mathbf{r}) + \rho_{0,\downarrow}(\mathbf{r}) = \rho_0(\mathbf{r})/2$. This sum rule is exact for the longitudi-

nal component, but neglects the very small Landau diamagnetic contribution for the transverse component.²⁵

The Kohn–Sham response functions can be expressed in closed form in terms of the unperturbed Kohn–Sham orbitals $\phi_{n\sigma}(\mathbf{r})$ and orbital energies $\epsilon_{n\sigma}$,

$$\begin{aligned} \chi_{AB}^{\sigma\sigma'}(\mathbf{r}, \mathbf{r}', \omega) &= \delta_{\sigma\sigma'} \sum_{n, n'} (f_{n\sigma} - f_{n'\sigma'}) \\ &\times \frac{\phi_{n\sigma}^*(\mathbf{r}) \hat{A} \phi_{n'\sigma'}(\mathbf{r}) \phi_{n'\sigma'}^*(\mathbf{r}') \hat{B} \phi_{n\sigma}(\mathbf{r}')}{(\epsilon_{n\sigma} - \epsilon_{n'\sigma'}) + \omega + i\eta}, \end{aligned} \quad (11)$$

where n and n' run over all states. In this equation the density operator $\hat{\rho} = 1$ and the paramagnetic current operator $\hat{\mathbf{j}} = -i(\nabla - \nabla^\dagger)/2$ can be substituted for the operators \hat{A} and \hat{B} , and the $f_{n\sigma}$ are the occupation numbers of the Kohn–Sham orbitals. The infinitesimal η ensures that the response function has the correct causal (retarded) structure. In the following we can set the infinitesimal η to zero because the spectrum is discrete below the ionization level, and as mentioned before we assume that there are no fractional occupation numbers. The response functions then become,

$$\begin{aligned} \chi_{AB}^{\sigma\tau}(\mathbf{r}, \mathbf{r}', \omega) &= \delta_{\sigma\tau} \sum_{i,a} \frac{\phi_{i\sigma}^*(\mathbf{r}) \hat{A} \phi_{a\tau}(\mathbf{r}) \phi_{a\tau}^*(\mathbf{r}') \hat{B} \phi_{i\sigma}(\mathbf{r}')}{(\epsilon_{i\sigma} - \epsilon_{a\tau}) + \omega} \\ &+ \frac{\phi_{i\sigma}(\mathbf{r}) \hat{A}^\dagger \phi_{a\tau}^*(\mathbf{r}) \phi_{a\tau}(\mathbf{r}') \hat{B}^\dagger \phi_{i\sigma}^*(\mathbf{r}')}{(\epsilon_{i\sigma} - \epsilon_{a\tau}) - \omega}, \end{aligned} \quad (12)$$

where i runs over the occupied states and a over the unoccupied states, σ and τ are the corresponding spin variables. We can express the total spin-integrated induced density and induced current density as follows:

$$\begin{aligned} \delta\rho(\mathbf{r}, \omega) &= \sum_{\sigma} \sum_{i,a} [\phi_{a\sigma}^*(\mathbf{r}) \phi_{i\sigma}(\mathbf{r}) P_{ai\sigma}(\omega) \\ &+ \phi_{i\sigma}^*(\mathbf{r}) \phi_{a\sigma}(\mathbf{r}) P_{ia\sigma}(\omega)], \end{aligned} \quad (13)$$

$$\begin{aligned} \delta\mathbf{j}(\mathbf{r}, \omega) &= \sum_{\sigma} \sum_{i,a} \left[\frac{-\omega}{(\epsilon_{i\sigma} - \epsilon_{a\sigma})} \phi_{a\sigma}^*(\mathbf{r}) \hat{\mathbf{j}} \phi_{i\sigma}(\mathbf{r}) P_{ai\sigma}(\omega) \right. \\ &\left. + \frac{-\omega}{(\epsilon_{i\sigma} - \epsilon_{a\sigma})} \phi_{i\sigma}^*(\mathbf{r}) \hat{\mathbf{j}} \phi_{a\sigma}(\mathbf{r}) P_{ia\sigma}(\omega) \right], \end{aligned} \quad (14)$$

where we define a so-called “ P -matrix,”

$$\begin{aligned} P_{ia\sigma}(\omega) &= \frac{1}{(\epsilon_{i\sigma} - \epsilon_{a\sigma}) - \omega} \left[\frac{-\omega}{(\epsilon_{i\sigma} - \epsilon_{a\sigma})} \right. \\ &\times \int \phi_{i\sigma}^*(\mathbf{r}) \hat{\mathbf{j}} \phi_{a\sigma}(\mathbf{r}) \delta\mathbf{A}_{\text{eff},\sigma}(\mathbf{r}, \omega) d\mathbf{r} \\ &\left. + \int \phi_{i\sigma}^*(\mathbf{r}) \delta v_{\text{eff},\sigma}(\mathbf{r}, \omega) \phi_{a\sigma}(\mathbf{r}) d\mathbf{r} \right], \end{aligned} \quad (15)$$

and we define $P_{ai\sigma}(\omega) = P_{ia\sigma}^*(-\omega)$. Inserting the definitions for $\delta\mathbf{A}_{\text{eff}}$ and δv_{eff} in Eq. (15) and substituting $\delta\rho$ and $\delta\mathbf{j}$ with Eqs. (13) and (14) we obtain,

$$\begin{aligned} P_{ia\sigma}(\omega) &= \frac{1}{(\epsilon_{i\sigma} - \epsilon_{a\sigma}) - \omega} \left[\frac{-\omega}{(\epsilon_{i\sigma} - \epsilon_{a\sigma})} \right. \\ &\times \int \phi_{i\sigma}^*(\mathbf{r}) \hat{\mathbf{j}} \phi_{a\sigma}(\mathbf{r}) \delta\mathbf{A}_{\text{ext},\sigma}(\mathbf{r}, \omega) d\mathbf{r} \\ &\left. + \sum_{jb\tau} (K_{ia,bj}^{\sigma\tau} P_{bj\tau}(\omega) + K_{ia,jb}^{\sigma\tau} P_{jb\tau}(\omega)) \right], \end{aligned} \quad (16)$$

where we have defined an in general frequency dependent coupling matrix,

$$\begin{aligned} K_{ia,jb}^{\sigma\tau}(\omega) &= \int \int \phi_{i\sigma}^*(\mathbf{r}) \phi_{a\sigma}(\mathbf{r}) \left[\frac{1}{|\mathbf{r} - \mathbf{r}'|} + f_{\text{xc}}^{\sigma\tau}(\mathbf{r}, \mathbf{r}', \omega) \right] \\ &\times \phi_{j\tau}(\mathbf{r}') \phi_{b\tau}^*(\mathbf{r}') d\mathbf{r} d\mathbf{r}' + \left(\frac{-\omega}{(\epsilon_{i\sigma} - \epsilon_{a\sigma})} \right)^2 \\ &\times \int \int \phi_{i\sigma}^*(\mathbf{r}) \hat{\mathbf{j}} \phi_{a\sigma}(\mathbf{r}) \mathbf{f}_{\text{xc}}^{\sigma\tau}(\mathbf{r}, \mathbf{r}', \omega) \\ &\times \phi_{j\tau}(\mathbf{r}') \hat{\mathbf{j}} \phi_{b\tau}^*(\mathbf{r}') d\mathbf{r} d\mathbf{r}'. \end{aligned} \quad (17)$$

Only if the adiabatic local density approximation (ALDA) is used for the scalar xc-kernel $f_{\text{xc}}^{\sigma\tau}$ and if for the tensor xc-kernel $\mathbf{f}_{\text{xc}}^{\sigma\tau}$ one approximates $\mathbf{f}_{\text{xc}}(\mathbf{r}, \mathbf{r}', \omega) = c(\mathbf{r}, \mathbf{r}')/\omega^2$, where $c(\mathbf{r}, \mathbf{r}') = \lim_{\omega \rightarrow 0} \omega^2 \mathbf{f}_{\text{xc}}(\mathbf{r}, \mathbf{r}', \omega)$ the coupling matrix becomes frequency independent. This is the approximation we will use in the sequel. We can rewrite the equations above and obtain the following set of linear equations:

$$\begin{aligned} \sum_{jb\tau} [\delta_{\sigma\tau} \delta_{ij} \delta_{ab} ((\epsilon_{a\sigma} - \epsilon_{i\sigma}) + \omega) + K_{ia,jb}^{\sigma\tau}] P_{jb\tau}(\omega) \\ + \sum_{jb\tau} K_{ia,bj}^{\sigma\tau} P_{bj\tau}(\omega) \\ = \frac{\omega}{(\epsilon_{i\sigma} - \epsilon_{a\sigma})} \int \phi_{i\sigma}^*(\mathbf{r}) \hat{\mathbf{j}} \phi_{a\sigma}(\mathbf{r}) \delta\mathbf{A}_{\text{ext},\sigma}(\mathbf{r}, \omega) d\mathbf{r} \end{aligned} \quad (18)$$

and

$$\begin{aligned} \sum_{jb\tau} [\delta_{\sigma\tau} \delta_{ij} \delta_{ab} ((\epsilon_{a\sigma} - \epsilon_{i\sigma}) - \omega) + K_{ai,bj}^{\sigma\tau}] P_{bj\tau}(\omega) \\ + \sum_{jb\tau} K_{ai,jb}^{\sigma\tau} P_{jb\tau}(\omega) \\ = \frac{\omega}{(\epsilon_{i\sigma} - \epsilon_{a\sigma})} \int \phi_{a\sigma}^*(\mathbf{r}) \hat{\mathbf{j}} \phi_{i\sigma}(\mathbf{r}) \delta\mathbf{A}_{\text{ext},\sigma}(\mathbf{r}, \omega) d\mathbf{r}. \end{aligned} \quad (19)$$

These equations may be compared with Eq. (14) on p. 124 of Ref. 21; the form of this equation is identical to Eqs. (18) and (19). Solving this set of linear equations can therefore proceed completely analogous to Ref. 21. The set of equations can be transformed to a set of equations for $P_{jb\tau} + P_{bj\tau}$ and $P_{jb\tau} - P_{bj\tau}$. One then obtains for $\delta P_{jb\tau} = (P_{jb\tau} + P_{bj\tau})/2$ an equation that is analogous to Eq. (22) on p. 125 of Ref. 21,

$$\begin{aligned}
& \sum_{jb\tau} \left[\delta_{\sigma\tau} \delta_{ab} \delta_{ij} (\epsilon_{i\sigma} - \epsilon_{a\sigma}) - 2K_{ia,jb}^{\sigma\tau} \right. \\
& \quad \left. - \omega^2 \frac{\delta_{\sigma\tau} \delta_{ab} \delta_{ij}}{(\epsilon_{i\sigma} - \epsilon_{a\sigma})} \right] \delta P_{jb\tau}(\omega) \\
& = \frac{\omega}{(\epsilon_{i\sigma} - \epsilon_{a\sigma})} \int \phi_{i\sigma}^*(\mathbf{r}) \hat{\mathbf{j}} \phi_{a\sigma}(\mathbf{r}) \delta \mathbf{A}_{\text{ext},\sigma}(\mathbf{r}, \omega) d\mathbf{r}, \quad (20)
\end{aligned}$$

the only difference being that our external perturbation has the form of a vector potential instead of a scalar potential and that the coupling matrix contains extra terms. In case of an excitation energy a finite external vector potential leads to an infinite change in the P matrix. This argument leads to the following eigenvalue equation from which the excitation energies and oscillator strengths can be obtained:

$$\Omega \mathbf{F}_n = \omega_n^2 \mathbf{F}_n, \quad (21)$$

where the ω_n are the excitation energies and the elements of \mathbf{F} are given by

$$F_{ia\sigma} = \frac{1}{\sqrt{\epsilon_{a\sigma} - \epsilon_{i\sigma}}} (P_{ia\sigma} + P_{ai\sigma}). \quad (22)$$

The oscillator strengths can be obtained from the eigenvectors \mathbf{F}_n . For a spin-restricted calculation the Ω matrix can be split into a singlet and triplet part by a unitary transformation giving for the components of the four-index matrices Ω^S and Ω^T ,

$$\begin{aligned}
\Omega_{ia,jb}^S &= \delta_{ij} \delta_{ab} (\epsilon_a - \epsilon_i)^2 + 2\sqrt{\epsilon_a - \epsilon_i} (K_{ia,jb}^{\uparrow\uparrow} + K_{ia,jb}^{\uparrow\downarrow}) \\
& \quad \times \sqrt{\epsilon_b - \epsilon_j}, \quad (23)
\end{aligned}$$

$$\begin{aligned}
\Omega_{ia,jb}^T &= \delta_{ij} \delta_{ab} (\epsilon_a - \epsilon_i)^2 + 2\sqrt{\epsilon_a - \epsilon_i} (K_{ia,jb}^{\uparrow\uparrow} - K_{ia,jb}^{\uparrow\downarrow}) \\
& \quad \times \sqrt{\epsilon_b - \epsilon_j}. \quad (24)
\end{aligned}$$

With the computational method outlined we are now ready to consider a particular form for the xc-kernel for the vector potential $\mathbf{f}_{xc}^{\sigma\tau}$.

B. The Vignale–Kohn functional and excitation spectra

For the spin independent case we have already explained our implementation of the Vignale–Kohn functional in detail in Ref. 13. Here we will explain the use of the Vignale–Kohn functional in case of the calculation of excitation spectra. For this it is necessary to consider the spin dependent case to arrive at expressions for the singlet and triplet excitations.

Before we consider the spin dependent VK functional for general systems, we consider first the case of the homogeneous electron gas. In this case $f_{xc}^{\sigma\sigma'}(\mathbf{r}, \mathbf{r}', \omega)$ and $\mathbf{f}_{xc}^{\sigma\sigma'}(\mathbf{r}, \mathbf{r}', \omega)$ merely depend on the separation $|\mathbf{r} - \mathbf{r}'|$. If we Fourier transform $\mathbf{f}_{xc}^{\sigma\sigma'}(\mathbf{r}, \mathbf{r}', \omega)$ with respect to $\mathbf{r} - \mathbf{r}'$ one arrives at the following form:

$$f_{xc,ij}^{\sigma\sigma'}(k, \omega) = \frac{1}{\omega^2} [f_{xcL}^{\sigma\sigma'}(k, \omega) k_i k_j + f_{xcT}^{\sigma\sigma'}(k, \omega) (k^2 \delta_{ij} - k_i k_j)]. \quad (25)$$

This defines the longitudinal and transverse xc-kernels $f_{xcL}^{\sigma\sigma'}(k, \omega)$ and $f_{xcT}^{\sigma\sigma'}(k, \omega)$. The small k expansion of these kernels is given by^{26,27}

$$f_{xcL(T)}^{\sigma\sigma'}(k, \omega) = \frac{A(\omega)}{k^2} \frac{\sigma\sigma' \rho_0^2}{4\rho_{0,\sigma}\rho_{0,\sigma'}} + B_{L(T)}^{\sigma\sigma'}(\omega) + O(k^2), \quad (26)$$

where the singular component $A(\omega)$ (in the $k \rightarrow 0$ limit) and the regular component $B_{L(T)}^{\sigma\sigma'}(\omega)$ are complex functions of the frequency, $\rho_0 = \rho_{0,\uparrow} + \rho_{0,\downarrow}$, and $\sigma = +1$ for spin-up and $\sigma = -1$ for spin-down. Note that for the spin restricted singlet excitations we need to sum over all spin variables, in that case the contribution of $A(\omega)$ vanishes.

It has been shown by Vignale, Ullrich, and Conti^{16,28} that the VK expression for the spin-independent case can be written in the form of a viscoelastic field. The spin dependent description of the VK functional is given by^{26,27}

$$\begin{aligned}
\delta \mathbf{E}_{xc,\sigma}(\mathbf{r}, \omega) &= \nabla \delta v_{xc,\sigma}^{\text{ALDA}}(\mathbf{r}, \omega) + i\omega \delta \mathbf{A}_{xc,\sigma}^{\text{viscoel}}(\mathbf{r}, \omega) \\
& \quad - \frac{i\rho_0(\mathbf{r})^2 A(\omega)}{4\omega} \\
& \quad \times \sum_{\sigma'} \frac{\sigma\sigma'}{\rho_{0,\sigma}(\mathbf{r})\rho_{0,\sigma'}(\mathbf{r})} \delta \mathbf{j}_{\sigma'}(\mathbf{r}, \omega). \quad (27)
\end{aligned}$$

The first two terms in this expression are the ALDA contribution and the viscoelastic force term. The former is obtained using the ALDA expression for the scalar xc-kernel,

$$f_{xc,\text{ALDA}}^{\sigma\tau}(\mathbf{r}, \mathbf{r}', \omega) = \delta(\mathbf{r} - \mathbf{r}') \left. \frac{\partial v_{xc,\text{LDA}}^\sigma}{\partial \rho_\tau} \right|_{\rho_\tau = \rho_{0,\tau}}, \quad (28)$$

while the latter is related to the viscoelastic stress tensor $\sigma_{xc,\sigma}(\mathbf{r}, \omega)$ by,

$$\delta A_{xc,\sigma,i}^{\text{viscoel}}(\mathbf{r}, \omega) = \frac{i}{\omega \rho_0(\mathbf{r})} \sum_j \partial_j \sigma_{xc,\sigma,ij}(\mathbf{r}, \omega), \quad (29)$$

$$\begin{aligned}
\sigma_{xc,\sigma,ij}(\mathbf{r}, \omega) &= \sum_{\sigma'} \{ \tilde{\eta}_{xc}^{\sigma\sigma'}(\mathbf{r}, \omega) [\partial_j u_{\sigma',i}(\mathbf{r}, \omega) \\
& \quad + \partial_i u_{\sigma',j}(\mathbf{r}, \omega) - \frac{2}{3} \delta_{ij} \nabla \cdot \mathbf{u}_{\sigma'}(\mathbf{r}, \omega)] \\
& \quad + \tilde{\xi}_{xc}^{\sigma\sigma'}(\mathbf{r}, \omega) \delta_{ij} \nabla \cdot \mathbf{u}_{\sigma'}(\mathbf{r}, \omega) \}. \quad (30)
\end{aligned}$$

In this expression $\mathbf{u}_{\sigma'}(\mathbf{r}, \omega) = \delta \mathbf{j}_{\sigma'}(\mathbf{r}, \omega) / \rho_{0,\sigma}(\mathbf{r})$ is the velocity field, in which $\delta \mathbf{j}_{\sigma'}(\mathbf{r}, \omega)$ is the induced current density. The coefficients $\tilde{\eta}_{xc}^{\sigma\sigma'}(\omega)$ and $\tilde{\xi}_{xc}^{\sigma\sigma'}(\omega)$ are related to the regular component of the xc-kernel of the homogeneous electron gas by the following relations:²⁶

$$\tilde{\eta}_{xc}^{\sigma\sigma'}(\omega) = - \frac{\rho_{0,\sigma}(\mathbf{r}) \rho_{0,\sigma'}(\mathbf{r})}{i\omega} B_T^{\sigma\sigma'}(\omega), \quad (31)$$

$$\begin{aligned}
\tilde{\xi}_{xc}^{\sigma\sigma'}(\omega) &= - \frac{\rho_{0,\sigma}(\mathbf{r}) \rho_{0,\sigma'}(\mathbf{r})}{i\omega} \\
& \quad \times \left(B_L^{\sigma\sigma'}(\omega) - \frac{4}{3} B_T^{\sigma\sigma'}(\omega) - \frac{\partial^2 \epsilon_{xc}}{\partial \rho_{0,\sigma} \partial \rho_{0,\sigma'}} \right), \quad (32)
\end{aligned}$$

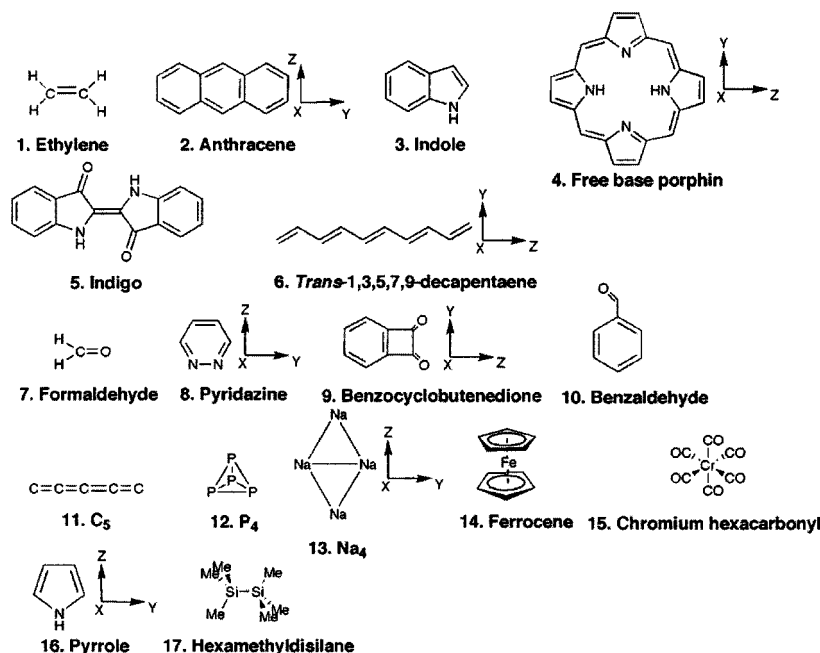


FIG. 1. Overview of the studied molecules with their structure and orientation in case there is an ambiguity.

where $\epsilon_{xc}(\rho_0)$ is the xc-energy per unit volume of the homogeneous electron gas of density ρ_0 . The third term in Eq. (27) is new in the spin dependent formulation and comes directly from the singular component of the xc-kernel of the homogeneous electron gas. The essential feature of this new term is that it produces damping of the spin-current proportional to the relative velocity between up- and down-spin electrons.²⁶ Similar to the response calculations^{12,13} we consider the coefficients $A(\omega)$ and $B(\omega)$ only in the static limit ($\omega \rightarrow 0$) for which the following exact results hold:²⁶ $\text{Im}A(\omega) \propto \omega^3$ and $\text{Re}A(\omega) \propto \omega^2$. In this limit the third term in Eq. (27) hence vanishes. For the regular component $B_{L(T)}^{\sigma\sigma'}(\omega)$ we have the exact relation²⁶ $\lim_{\omega \rightarrow 0} \{ (B_{L(T)}^{\sigma\sigma'}(\omega) - 4B_T^{\sigma\sigma'}(\omega)/3 - \partial^2 \epsilon_{xc} / \partial \rho_{0,\sigma} \partial \rho_{0,\sigma'}) / \omega \} = 0$, hence the coefficient $\omega \tilde{\eta}_{xc}^{\sigma\sigma'}(\omega)$ also vanishes in this limit.

For the singlet and triplet excitations as derived from Eqs. (23) and (24) we need to consider the following singlet and triplet combinations of the $\tilde{\eta}_{xc}^{\sigma\sigma'}(\omega)$:

$$\tilde{\eta}_{xc}^S(\omega) = - \sum_{\sigma\sigma'} \frac{\rho_{0,\sigma}(\mathbf{r})\rho_{0,\sigma'}(\mathbf{r})}{i\omega} B_T^{\sigma\sigma'}(\omega), \quad (33)$$

$$\tilde{\eta}_{xc}^T(\omega) = - \sum_{\sigma\sigma'} \sigma\sigma' \frac{\rho_{0,\sigma}(\mathbf{r})\rho_{0,\sigma'}(\mathbf{r})}{i\omega} B_T^{\sigma\sigma'}(\omega), \quad (34)$$

respectively, called the density–density and spin–spin channels by Qian, Constantinescu, and Vignale.²⁷ The $\tilde{\eta}_{xc}^S(\omega)$ is identical to the $\tilde{\eta}_{xc}(\omega)$ of the spin-independent case which we used before in our response calculations.^{12,13} In the static limit an expression for $\tilde{\eta}_{xc}^T(\omega)$ can be derived in terms of the Landau parameters of the electron gas.²⁷ In this article we will focus on the singlet excitations, and postpone the discussion of the triplet to a forthcoming article.

The VK functional is, if one wants to be consistent with the derivation of the VK functional,^{14,15} to be used in conjunction with the local density approximation for the ground-state calculation.

III. COMPUTATIONAL DETAILS

We want to test the performance of the VK-functional for different types of excitations. For this purpose we use the benchmark set devised by Parac and Grimme¹⁹ and augment it with the prototype $\pi^* \leftarrow \pi$ excitation in ethylene, the prototype $\pi^* \leftarrow n$ transition in formaldehyde and the 1^1B_u $\pi^* \leftarrow \pi$ transition in *trans*-1,3,5,7,9-decapentaene as an example of a molecular chain as we studied in Refs. 12 and 13. The molecules are shown in Fig. 1.

All calculations were performed with our modified version of ADF.^{29–34}

We optimized the geometries within the standard ADF TZ2P basis set, which is a triple zeta Slater-type basis set augmented with two polarization functions. Cores were kept frozen for carbon, oxygen, and nitrogen up to $1s$ and for phosphorus, sodium, silicon, chromium, and iron up to $2p$. Geometry optimizations were performed with a generalized gradient approximated potential (GGA) by Becke³⁵ for exchange and Perdew³⁶ for correlation (BP functional).

For the excitation energy calculations a larger basis set was used. We used the standard ADF ET-pVQZ basis, which is an even tempered Slater-type basis set of quadruple zeta quality. For pyrrole and hexamethyldisilane, for which we will study Rydberg-type excitations, we used the standard ADF ET-QZ3P-1DIFFUSE basis, which is an even tempered Slater-type basis set of quadruple zeta quality with diffuse functions. For the beryllium atom we used a very large even-tempered basis set called DIFFUSE10 which can be obtained via Ref. 29. This basis is close to the basis set limit.

TABLE I. This table shows the excitation energies of transitions with $\pi^* \leftarrow \pi$ character. All values are in eV.

Molecule	State	Expt.	MR -MP2 ^a	CC2 ^a	Other theory	LDA/ ALDA	LDA/ VK
(1) C ₂ H ₄	1 ¹ B _{1u}	7.66 ^b			7.94, ^c 7.89 ^d	7.55	8.05
(2) C ₁₄ H ₁₀	1 ¹ B _{1u} (L _a)	3.31, ^e 3.43 ^f	3.69	3.99	4.57 ^h	2.86	3.53
	1 ¹ B _{2u} (L _b)	3.45, ^g 3.47 ^f	3.35	3.93	5.29 ^h	3.57	3.61
(3) C ₈ H ₇ N	2 ¹ A' (L _b)	4.37 ⁱ	4.25	4.93	4.43 ^j	4.34 ^k	4.66
	3 ¹ A' (L _a)	4.77 ^j	4.95	4.33	4.73 ^j	4.59 ^k	4.74
(4) C ₂₀ H ₁₄ N ₄	1 ¹ B _{1u} (Q _x)	1.98–2.02 ^l	1.67	2.32	1.63 ^m	2.18	2.23
	1 ¹ B _{2u} (Q _y)	2.33–2.42 ^l	2.33	2.71	2.11 ^m	2.30	2.34
	2 ¹ B _{2u} (B _y)	3.13–3.33 ^m	3.28	3.66	3.08 ^m	2.99	3.10
	2 ¹ B _{1u} (B _x)	3.13–3.33 ^m	3.08	3.57	3.12 ^m	2.97	3.45
(5) C ₁₆ H ₁₀ N ₂ O ₂	1 ¹ B _u	2.30 ⁿ	2.10	2.36	1.96 ^o	1.93	2.89
(6) C ₁₀ H ₁₂	1 ¹ B _u	4.02 ^p			4.33, ^q 4.05 ^r	3.26	4.33

^aReference 19.^bReference 38.^cMR-SDCI results from Ref. 39.^dEOM-CCSDT-3 results from Ref. 41.^eReference 45, in *n*-heptane solution.^fReference 47, these are the (extrapolated) results for the *free* molecule.^gReference 46, in cyclohexane.^hCASSCF results from Ref. 48.ⁱReference 49.^jCASPT2 results from Ref. 50.^kThe character of these states is L_a for the 2 ¹A' state and L_b for the 3 ¹A' state.^lFrom Ref. 53, Ref. 75, and Ref. 76.^mCASPT2 results from Ref. 77.ⁿVapor spectra from Ref. 54.^oCASPT2 results from Ref. 55.^pGas phase measurements from Ref. 56.^qCIS results from Ref. 58.^rMRMP results from Ref. 57, these values are corrected for the basis set and active space effects.

In all excitation energy calculations the ground state has been calculated with the LDA functional in the VWN parameterization.³⁷ The response calculations themselves were done with the standard adiabatic local density approximation (ALDA) and the Vignale–Kohn functional (VK). From now on we denote these calculations simply as ALDA and VK instead of LDA/ALDA and LDA/VK.

In the excitation energy calculations the numerical integration accuracy was set to at least five decimals.

IV. RESULTS

In the following we will discuss our results for the benchmark set. We have divided this part into three main sections. The first section contains the $\pi^* \leftarrow \pi$ transitions, the second section the $\pi^* \leftarrow n$ transitions, and the final section contains the remaining transitions in the benchmark set. The reason for this division is that it turns out that the $\pi^* \leftarrow \pi$ and $\pi^* \leftarrow n$ transitions form distinct classes as far as the behavior of the VK functional is concerned.

A. $\pi^* \leftarrow \pi$ transitions

The results for the $\pi^* \leftarrow \pi$ transitions is shown in Table I.

1. Ethylene

The prototype of a $\pi^* \leftarrow \pi$ transition is the transition to the 1 ¹B_{1u} state in ethylene (known as the V–N transition). It turns out that the experimental value of 7.66 eV (Ref. 38) is difficult to reproduce even with highly accurate *ab initio*

wave function methods (for a discussion and references, see Ref. 39). It is generally agreed that this experimental value does not correspond to a vertical transition.⁴⁰ Therefore a theoretical estimate of 8 eV is generally used to compare results with.^{41,42} Davidson and Jarzęcki⁴³ derived equations to relate the vertical excitation to the average energy of the observed value. They obtain a value of 7.8 eV for the 1 ¹B_{1u} state. The multireference singles-doubles configuration interaction (MR-SDCI) results of 7.94 eV calculated by Lindh and Roos³⁹ and the more recent equation of motion singles doubles triples coupled cluster results (EOM-CCSDT-3, where the 3 means that an iterative method is used for the triple excitations) by Watts, Gwaltney, and Bartlett⁴¹ of 7.89 eV lie close to these values. We obtain a value of 7.55 eV with the ALDA and a value of 8.05 eV with VK. The VK value corrects for the underestimation of the ALDA result and we obtain a value in reasonable agreement with the estimates for the experimental value.

2. Anthracene

For anthracene we focus on two transitions of $\pi^* \leftarrow \pi$ character, the HOMO→LUMO transition (L_a band in Platt's notation⁴⁴) and the transition resulting from the nearly degenerate HOMO–1→LUMO and HOMO→LUMO+1 states (L_b band in Platt's notation). The absorption spectrum of anthracene^{45–47} shows that the transition to the 1 ¹B_{2u} state (L_b band) is hidden under the more intense 1 ¹B_{1u} state (L_a band). Using two-photon spectra the L_b band could be assigned with more certainty (see Ref. 47 for a discussion on

this matter). Wolf and Hollneicher⁴⁷ did measurements on anthracene in several solvents, from this they found the solvent shift and extrapolated their values to the free molecule. This shows that the splitting between the L_a and L_b band in the free molecule should be very small. Our VK results also show a small splitting and the values are also in good agreement with experiment and other theoretical values. The ALDA results give a splitting that is too large and the position of the L_a band is underestimated with ALDA, while the position of the L_b band is already in reasonable agreement with experiment. The order of the transitions is predicted correctly with TDDFT contrary to the CC2 (Ref. 19) and MR-MP2 (Ref. 19) results. The CASSCF (Ref. 48) results strongly overestimate the excitation energies.

3. Indole

For indole we again focus on the L_a ($3^1A'$) and L_b ($2^1A'$) bands. The VK results for the L_b and L_a bands are in good agreement with experiment⁴⁹ and CASPT2 (Ref. 50) results. The ALDA results for the $2^1A'$ state and the $3^1A'$ state are also in good agreement, but the ALDA assigns the $2^1A'$ state to the HOMO→LUMO transition (L_a) and the $3^1A'$ state to a transition consisting of contributions from HOMO−1→LUMO and HOMO→LUMO+1 transitions (L_b). The ALDA thus predicts the wrong ordering of the transitions. The VK corrects for this by giving the correct character without changing the energies too much.

4. Free base porphyrin

An extensive study of free base porphyrin (FBP) with TD-DFT has already been performed using ADF by van Gisbergen *et al.*⁵¹ They studied the excitation energies using the LDA, the BP xc-functional and the Van Leeuwen/Baerends model xc-potential (LB94) (Ref. 52) in the ground-state part of their calculations. From this study it turned out that there was not much difference between the results obtained with the different ground-state functionals. They found that the BP results support the interpretation of the spectrum by Edwards *et al.*⁵³ and the CASPT2 interpretation.⁵⁰ We will discuss how the VK functional affects these results. Like the study by Parac and Grimme,¹⁹ we studied the first four excitation energies. The lowest two form the Q bands of experiment. After these two distinct bands, the spectrum shows a broad band with a distinct shoulder. These are called the B and N bands. There is still much debate on the assignment of these higher excitations. More information about this and references can be found in Ref. 51. Since the purpose of this paper is to see how well VK performs, we will not discuss the assignment of the two higher excitations.

The lowest two Q bands are called Q_x and Q_y according to their polarization. These bands are formed by the transition to the 1^1B_{1u} and 1^1B_{2u} states. The VK functional does not have a big effect on the excitation energies of these states compared to the ALDA. The splitting between the states is small with VK just like with the ALDA. The splitting is 0.11 eV with VK. The experimental gas phase splitting is 0.44 eV.

The energy of the 2^1B_{2u} state is hardly affected by going from ALDA to VK while the energy of the 2^1B_{1u} state is

raised in energy by almost 0.5 eV with VK. The VK value for these states lie close to the experimental values for the broad B band.

5. Indigo

The lowest $\pi^* \leftarrow \pi$ transition in indigo is the transition to the 1^1B_u state. The ALDA underestimates the experimental value of 2.30 eV (Ref. 54) by 0.37 eV. The VK shifts this excitation energy upward, but the correction is too large leading to an overestimation compared to the experimental value (by 0.59 eV) and the other theoretical results.^{19,55}

6. *Trans*-1,3,5,7,9-decapentaene

In our previous studies^{12,13} we saw that the VK corrects the large overestimation of the static polarizability of oligomer chains obtained by the ALDA. It is expected that the VK functional will also have a large effect on the excitation energies of these systems. In a forthcoming article we will study the excitation energies of these oligomers in more detail. Here we will focus on *trans*-1,3,5,7,9-decapentaene. For this molecule experimental values⁵⁶ and MRMP (Ref. 57) and CIS (Ref. 58) results are available, while we observed already in this short chain a correction by VK of the static polarizability. The ALDA considerably underestimates the excitation energy for this molecule (more than 1 eV). The VK corrects the underestimation and we obtain a value equal to the CIS result, which lies close to the experimental and MRMP values.

B. Discussion of the $\pi^* \leftarrow \pi$ transitions

In nearly all cases studied we see an improvement by using the VK functional, with indigo being the only exception where there is an overestimation by VK of 0.59 eV which is larger than the underestimation by the ALDA of 0.37 eV. The correction is most profound for the molecular chain *trans*-1,3,5,7,9-decapentaene, where we observe an increase of 1.7 eV for the 1^1B_u in going from ALDA to VK, the VK value being close to experiment and other theory. Another nice result of the VK functional is that it gives the correct ordering of the L_a and L_b states for indole, contrary to the ALDA.

Until now we have not looked explicitly at the oscillator strengths. All the $\pi^* \leftarrow \pi$ excitations studied are dipole allowed and have finite oscillator strength. In Table II we show the oscillator strengths for the various transitions together with the absolute difference in excitation energy obtained with ALDA and VK, $|\Delta E^{\text{ALDA-VK}}|$. We also give the transition dipole moments and their orientation. If one looks, for example, at the four excitations of porphyrin, it can be seen that the larger the ALDA oscillator strength the larger the effect of VK on this transition. This trend can also be observed for the excitations of anthracene and indole. More generally we can state that the larger the transition dipole moment obtained within the ALDA is along the long axis of the molecule the larger the VK correction will be for that excitation. In case of porphyrin this is true for both the y and z direction. This indicates that the larger the current in the axial molecular direction the larger the VK correction. This

TABLE II. Oscillator strengths, transition dipole moments, and their correlation to the difference between the ALDA and VK excitation energies for the $\pi^* \leftarrow \pi$ transitions. The direction of the transition dipole moment is denoted in *italic*. All values are in eV.

Molecule	State	Oscillator strengths (a.u.)		Transition dipole moments (a.u.)		$ \Delta E^{\text{ALDA-VK}} $
		ALDA	VK	ALDA	VK	
(1) C ₂ H ₄	1 ¹ B _{1u}	0.32	0.32	1.31 <i>z</i>	1.29 <i>z</i>	0.50
(2) C ₁₄ H ₁₀	1 ¹ B _{1u}	0.033	0.019	0.69 <i>z</i>	0.47 <i>z</i>	0.68
	1 ¹ B _{2u}	<0.001	<0.001	0.039 <i>y</i>	0.078 <i>y</i>	0.05
(3) C ₈ H ₇ N	2 ¹ A'	0.050	0.006	0.46 <i>x</i> ; 0.51 <i>y</i>	0.20 <i>x</i> ; 0.11 <i>y</i>	0.32
	3 ¹ A'	0.017	0.035	0.37 <i>x</i> ; 0.11 <i>y</i>	0.42 <i>x</i> ; 0.36 <i>y</i>	0.15
(4) C ₂₀ H ₁₄ N ₄	1 ¹ B _{1u}	<0.001	<0.001	0.12 <i>z</i>	0.026 <i>z</i>	0.05
	1 ¹ B _{2u}	0.001	<0.001	0.14 <i>y</i>	0.041 <i>y</i>	0.04
	2 ¹ B _{2u}	0.034	<0.001	0.68 <i>y</i>	0.035 <i>y</i>	0.11
(5) C ₁₆ H ₁₀ N ₂ O ₂	2 ¹ B _{1u}	0.11	0.004	1.26 <i>z</i>	0.22 <i>z</i>	0.48
	1 ¹ B _u	0.22	0.13	2.07 <i>x</i> ; 0.65 <i>y</i>	1.30 <i>x</i> ; 0.38 <i>y</i>	0.96
(6) C ₁₀ H ₁₂	1 ¹ B _u	1.78	1.50	4.71 <i>x</i> ; 0.28 <i>y</i>	3.75 <i>x</i> ; 0.15 <i>y</i>	1.07

may indicate that the VK functional is able to include for these excitations the counteracting field that the ALDA fails to describe.

C. $\pi^* \leftarrow n$ transitions

The results for the $\pi^* \leftarrow n$ transitions are shown in Table III.

1. Formaldehyde

The prototype of a $\pi^* \leftarrow n$ transition is the transition to the 1 ¹A₂ state in formaldehyde. This state has a clear valence character and can be clearly identified in the absorption spectrum. The coupled-cluster CCSD value is 4.04 eV.⁵⁹ Our calculations give a value of 3.68 eV for ALDA and 8.34 eV for VK for this transition. This is a large overestimation by VK.

TABLE III. This table shows the excitation energies of transitions with $\pi^* \leftarrow n$ character. All values are in eV.

Molecule	State	Expt.	MR-		Other theory	LDA/ALDA	LDA/VK
			MP2 ^a	CC2 ^a			
(1) H ₂ CO	1 ¹ A ₂	3.79; ^b 4.07 ^c			4.04 ^d	3.68	8.34
(2) C ₄ H ₄ N ₂	1 ¹ B ₁	3.30 ^e	3.62	3.87	3.48 ^f	2.95	7.03
(3) C ₈ H ₄ O ₂	1 ¹ B ₁	2.79 ^g	2.68	2.99		2.01	4.67
	1 ¹ A ₂	3.49 ^g	3.62	3.83		2.76	5.27
(4) C ₇ H ₆ O	1 ¹ A''	3.8 ^h	3.98	3.92	3.71 ⁱ	3.08	4.46
(5) C ₅	1 ¹ Π _u	2.78 ^j	2.61	3.35	2.90 ^j	2.50	6.74

^aReference 19.

^bElectron impact spectroscopy values from Ref. 78.

^cReference 68.

^dCCSD results from Ref. 59.

^eReference 60.

^fCASPT2 results from Ref. 79.

^gAbsorption spectra in *n*-hexane solution from Ref. 61.

^hThis value is estimated on the basis of the experimentally obtained band origin (at 3.34 eV, Ref. 62) and the CASPT2 difference between the vertical and adiabatic transition (3.71 eV–3.27 eV=0.44 eV, Ref. 63).

ⁱCASPT2 results from Ref. 63.

^jGas phase measurements by Motylewski, Vaizert, and Giezen and MRCI results from Ref. 64.

2. Pyridazine

The lowest excitation in pyridazine is the transition to the 1 ¹B₁ state. This excitation has been experimentally found at 3.30 eV.⁶⁰ The ALDA underestimates this value by 0.35 eV. The VK functional overestimates strongly with a value of 7.03 eV.

3. Benzocyclobutenedione

The $\pi^* \leftarrow n$ transitions to the 1 ¹B₁ and 1 ¹A₂ states have been observed for benzocyclobutenedione in *n*-hexane solution.⁶¹ The ALDA again underestimates the experimental and theoretical values. The VK functional leads to an overestimation by more than 2 eV for both excitations.

4. Benzaldehyde

For benzaldehyde the vertical transition to the 1 ¹A'' state is not directly observed. A value of 3.8 eV is estimated on the basis of the experimentally obtained band origin⁶² and the CASPT2 difference between the vertical and adiabatic transitions.⁶³ The ALDA underestimates this value by 0.72 eV and also underestimates the other theoretical results. The VK functional overestimates by 0.66 eV.

5. C₅

As the final example of a $\pi^* \leftarrow n$ transition the transition to the 1 ¹Π_u state of the highly unsaturated C₅ molecule is studied. The ALDA underestimates the experimental value⁶⁴ by 0.28 eV. The VK functional overestimates this value by more than 3 eV.

D. Discussion of the $\pi^* \leftarrow n$ transitions

All the $\pi^* \leftarrow n$ transitions are strongly overestimated by the Vignale–Kohn functional except for benzaldehyde for which the overestimation is not as severe. For a more in depth look at the effect of the VK functional for these excitations we consider the matrix elements of the contribution of the xc-vector potential to the Hamiltonian, $\langle \phi_i | \mathbf{j} \cdot \mathbf{A}_{xc} | \phi_a \rangle$. It turns out that these matrix elements become excessively large for these transitions. This is unlike the $\pi^* \leftarrow \pi$ case.

TABLE IV. This table shows the excitation energies of transitions with various character, see the text for more detail. All values are in eV.

Molecule	State	Expt.	MR		Other theory	LDA/ALDA	LDA/VK
			-MP2 ^a	CC2 ^a			
(1) P ₄	1 ¹ T ₂	5.6 ^b	5.38	5.52		5.15	5.69
(2) Na ₄	1 ¹ B _{1u}	1.81 ^c	1.85	1.83	1.74 ^d	1.79	2.60
(3) C ₁₀ H ₁₀ Fe	1 ¹ E _{1g}	2.81 ^e	2.85	2.65		2.93	5.17
(4) Cr(CO) ₆	1 ¹ T _{1u}	4.43 ^f	4.56	3.96	4.54–4.11 ^g	4.14	4.62
	2 ¹ T _{1u}	5.41 ^f	5.42	4.36	5.07–5.20 ^g	5.68	6.31
(5) C ₄ H ₅ N	1 ¹ A ₂	5.22 ^h	5.26	5.14	5.10 ^j	4.81	5.04
	1 ¹ B ₁	5.86 ⁱ	6.00	5.80	5.85 ^j	5.20	5.29
(6) Si ₂ (CH ₃) ₆	1 ¹ E _u	6.35 ^k	6.52	5.72		5.32	5.55

^aReference 19.^bAbsorption spectra in solid argon from Ref. 65.^cPhotodepletion spectra from Ref. 80.^dCl results from Ref. 81.^eAbsorption spectra from Ref. 66.^fVapor spectra from Ref. 67.^gCASPT2 results from Ref. 82.^hReference 68.ⁱVapor spectra from Ref. 69.^jCC3 results from Ref. 83.^kElectron energy loss spectra from Ref. 70.

E. Miscellaneous transitions

The remaining results are given in Table IV. As an example of a system having excitations involving σ orbitals the covalently bound P₄ cluster and the metallic Na₄ cluster are studied. As a severe test some low-lying excited states involving d orbitals of the transition metal complexes ferrocene and chromiumhexacarbonyl are considered. Finally we study Rydberg states in pyrrole and hexamethyldisilane.

1. P₄

The first dipole-allowed transition in P₄ is the transition to the 1 ¹T₂ state. It is experimentally located at 5.6 eV.⁶⁵ The ALDA underestimates this value by 0.45 eV, but the VK corrects to a value of 5.69 eV. This value is very close to the experiment.

2. Na₄

The optically allowed 1 ¹B_{1u} state of the Na₄ cluster is another example of a system involving σ orbitals. Only in this case the system contains only metal atoms. The experimental excitation energy is located at 1.81 eV. The ALDA value of 1.79 eV lies very close to this value. The VK overestimates by 0.8 eV.

3. Ferrocene

For ferrocene in the D_{5d} symmetry the transition to the 1 ¹E_{1g} state is studied. The experimentally found value for this transition is 2.81 eV.⁶⁶ The ALDA results are reasonably close to the experiment and other theoretical results. The VK strongly overestimates by more than 2 eV.

4. Chromiumhexacarbonyl

Another example of a transition metal compound is chromiumhexacarbonyl. Two $\pi^* \leftarrow d$ charge transfer excitations are present in the test set. These excitations appear in the spectra⁶⁷ as two strong bands with maxima at 4.43 eV

and 5.41 eV. The ALDA underestimates the transition to the 1 ¹T_{1u} state and overestimates the transition to the 2 ¹T_{1u} state. The VK again shifts these excitation energies to higher values. The excitation energy for the 1 ¹T_{1u} state obtained with VK is in good agreement with the experiment and other theoretical values (except for CC2 which underestimates both excitations¹⁹). The 2 ¹T_{1u} excitation is already overestimated by the ALDA and the VK functional makes this even worse.

5. Pyrrole

For pyrrole the first two low-lying Rydberg-type transitions are studied. These are experimentally observed at 5.22 eV (Ref. 68) and 5.86 eV.⁶⁹ The ALDA underestimates these values and the other theoretical results. The VK increases the ALDA values but not enough; the VK values still underestimate the experiment.

6. Hexamethyldisilane

Another example of a Rydberg excitation is the transition to the 1 ¹E_u state in hexamethyldisilane. The experimentally found value is 6.35 eV.⁷⁰ With the ALDA we find 5.32 eV which is an underestimation of more than 1 eV. With VK this value is raised to 5.55 eV, which is still a strong underestimation.

V. Discussion of the miscellaneous transitions

Except for the case of ferrocene the excitation energy shifts due to VK are moderate sometimes improving, sometimes worsening the results. The shift due to VK is upward in all cases. Except for the transition to the 2 ¹T_{1u} state in chromiumhexacarbonyl and the transition to the 1 ¹E_{1g} state of ferrocene the ALDA always underestimates. The too high excitation energies cannot be corrected by including a counteracting field term through the VK functional. The VK shift in the transition metal complex chromiumhexacarbonyl is not very large, contrary to the case of ferrocene for which the transition to the 1 ¹E_{1g} state is strongly overestimated by VK. The Rydberg excitation energies are still underestimated with VK, but it should be noted that for these excitations use of an asymptotically correct functional such as the LB94 (Ref. 52) functional is necessary to obtain good results. A large correction is not necessary for these systems if the LB94 is used in the ground state, indicating that the fact that VK does not correct the ALDA a lot in case of the Rydberg states is not a failure of the VK.

V. CONCLUSION

In this paper we have shown that the TDCDFT approach which we used before to obtain polarizabilities can be reformulated to describe the excitation spectrum in a way analogous to the ordinary TDDFT approach. The final equations are of similar form in which only the coupling matrix in the TDCDFT case contains extra terms involving a tensor xc-kernel. For this tensor xc-kernel we used the Vignale–Kohn approximation.

We applied this method to a benchmark set of molecules and considered excitations of various nature. The $\pi^* \leftarrow \pi$ ex-

citation energies obtained with VK improve the ALDA results in all cases except indigo. This is in line with the results obtained for the polarizabilities in the π -conjugated systems.^{12,13} For the $\pi^* \leftarrow n$ excitation energies and the transition to the 1^1E_{1g} state of ferrocene the VK dramatically fails. For the other type of excitations contained in the benchmark set no clear picture emerged: sometimes the VK improves and sometimes it worsens upon the ALDA, but in general no large effects were observed.

A possible explanation that the VK functional behaves differently for different kinds of transitions may be found in the fact that the functional is derived for a system that is very different from the ones we study. The VK functional was derived by an expansion to second order in wave vectors k and q , which characterize the Fourier component of the current-current response function for the electron gas and the wavelength of the inhomogeneity, respectively. This expansion was shown to be valid in the regime $k, q \ll k_F, \omega/v_F$ where k_F is the Fermi momentum and v_F the Fermi velocity of the electron gas. This is the region above the particle-hole continuum. For the wave vector of the applied optical field the constraints $k \ll k_F, \omega/v_F$ are trivially met as $k = \omega/c \ll k_F$, and the speed of light $c \gg v_F$. However, since we consider excitations in molecular systems, the self-consistent perturbing field associated with a given excitation will vary on a length scale that is determined by the inhomogeneity of the induced density and current density describing the excitation, and hence by the particular orbital structure of the transitions involved. An optimistic estimate for this perturbing field will be $k \approx 2\pi/L$, with L the characteristic size of the molecule, but a more realistic value would be to consider $k \approx q$, i.e., of the same order as the inhomogeneity. For the wave vector characterizing the inhomogeneity of the ground-state density, we have $q = |\nabla\rho_0|/\rho_0$. In the core and valence region q is of the same order as k_F and $1/v_F$,^{52,71} whereas in the asymptotic outer region $q \gg k_F$ and $q \ll 1/v_F$. The constraints on the wave vector q are violated, although not strongly, almost everywhere in the molecule, while the extent of the violation of the constraints on k will depend on the particular excitation considered.

One should keep in mind that meeting the constraints on k and q in itself does not justify the use of an xc-functional derived for the weakly inhomogeneous metallic electron gas to inhomogeneous systems with an excitation gap. This problem is not unique to the VK functional, but is already present for the local density approximation and for the gradient corrections. However, the VK functional satisfies two important constraints, which are valid for systems with arbitrary time dependence and inhomogeneity (such as molecules in external fields), stating that in linear response the xc-electric field does not exert any forces or torques on the system. Another exact property, which is satisfied for any system, is that under rigid translation of the center of mass, described by position vector $\mathbf{x}(\omega)$, the xc-potential is also translated over this vector. This immediately implies that the VK functional satisfies the so-called harmonic potential theorem.^{72,73} In view of these exact properties one may hope that the VK functional is still applicable to the inhomogeneous systems with an excitation gap such as molecules. The particle-hole re-

TABLE V. This table shows the lowest two excitation energies of transitions for the beryllium atom. All values are in eV.

Transition	Expt. ^a	ALDA results by Ullrich ^b	VK results by Ullrich ^b	LDA/ALDA	LDA/VK
$2s \rightarrow 2p$	5.27	5.07	6.24	4.86	5.62
$2s \rightarrow 3s$	6.77	5.62	5.67	5.65	6.63

^aReference 84.

^bReference 74.

gime, for which the VK derivation is not justified, is to a large extent taken into account by the explicit evaluation of the Kohn-Sham response functions.

It is our observation that for the $\pi^* \leftarrow \pi$ transitions the results obtained are much improved when including the VK contribution to the exchange-correlation potentials. For the $\pi^* \leftarrow \pi$ transitions the region where the xc-field contributes most to the matrix elements is neither close to the nuclei nor in the remote outer region: the induced current associated with such transitions is mainly in the π -system in the direction of the long axis of the molecules, and it is more or less uniform along this axis. Even though the equilibrium density is far from homogeneous ($q \approx k_F$) in the relevant region, the density gradient is mostly in a direction perpendicular to the induced current. We may speculate that this remnant of a weak inhomogeneity might result in the xc-functional to behave in a graceful manner. A similar argument cannot be used for the $\pi^* \leftarrow n$ transitions, for which we observe that the VK functional severely fails to describe these transitions correctly. The systems studied are however too complicated to analyze this conjecture. We propose to study simpler systems, that are chemically relevant, and that can be analyzed to a larger extent. As turns out the VK functional also fails for some transitions in atoms. Ullrich and Burke has done an independent study of excitation energies of atoms with the VK functional. They obtained excitation energies using the so-called single pole approximation, in which only the diagonal elements of the coupling matrix are included. Their (unpublished) results⁷⁴ show that also in the case of atoms there are certain excitations that are strongly overcorrected by VK while others remain nearly unchanged. For example in case of beryllium (Table V) the $2p \leftarrow 2s$ excitation energy is strongly overestimated by VK, while the $3s \leftarrow 2s$ excitation energy is shifted only slightly by VK, improving over the ALDA result. We see a similar effect for our implementation of the VK functional, which takes into account all matrix elements of the coupling matrix: the large shift observed for the $2p \leftarrow 2s$ excitation energy in the single pole approximation is reduced by taking into account off diagonal elements but it is still 0.35 eV too large. For the $3s \leftarrow 2s$ excitation both methods find a small shift. We hope to gain more insight in the range of applicability of the VK functional in molecules, and to find the cause of its failure for particular transitions, by studying atoms in more detail.

ACKNOWLEDGMENTS

We gratefully acknowledge Carsten Ullrich and Kieron Burke for providing us with their unpublished data on the use of the VK functional for beryllium and other atoms. We also thank Robert van Leeuwen for many valuable discussions, and especially Jaap G. Snijders (2003†) who initiated this project and who was closely involved during its early stages.

- ¹E. Runge and E. K. Gross, *Phys. Rev. Lett.* **52**, 997 (1984).
- ²E. K. U. Gross and W. Kohn, *Adv. Quantum Chem.* **21**, 255 (1990).
- ³R. van Leeuwen, *Int. J. Mod. Phys. B* **15**, 1969 (2001).
- ⁴B. Champagne, E. A. Perpète, S. J. A. van Gisbergen, E. J. Baerends, J. G. Snijders, C. Soubra-Ghaoui, K. A. Robins, and B. Kirtman, *J. Chem. Phys.* **109**, 10489 (1998).
- ⁵S. J. A. van Gisbergen, P. R. T. Schipper, O. V. Gritsenko, E. J. Baerends, J. G. Snijders, B. Champagne, and B. Kirtman, *Phys. Rev. Lett.* **83**, 694 (1999).
- ⁶J. D. Talman and W. G. Shadwick, *Phys. Rev. A* **14**, 36 (1976).
- ⁷P. Mori-Sanchez, Q. Wu, and W. T. Yang, *J. Chem. Phys.* **119**, 11001 (2003).
- ⁸Y. H. Kim and A. Görling, *Phys. Rev. B* **66**, 035114 (2002).
- ⁹J. B. Krieger, Y. Li, and G. J. Iafrate, *Phys. Rev. A* **45**, 101 (1992).
- ¹⁰M. Grüning, O. V. Gritsenko, and E. J. Baerends, *J. Chem. Phys.* **116**, 6435 (2002).
- ¹¹F. Della Sala and A. Görling, *J. Chem. Phys.* **115**, 5718 (2001).
- ¹²M. van Faassen, P. L. de Boeij, R. van Leeuwen, J. A. Berger, and J. G. Snijders, *Phys. Rev. Lett.* **88**, 186401 (2002).
- ¹³M. van Faassen, P. L. de Boeij, R. van Leeuwen, J. A. Berger, and J. G. Snijders, *J. Chem. Phys.* **118**, 1044 (2003).
- ¹⁴G. Vignale and W. Kohn, *Phys. Rev. Lett.* **77**, 2037 (1996).
- ¹⁵G. Vignale and W. Kohn, in *Electronic Density Functional Theory: Recent Progress and New Directions*, edited by J. F. Dobson, G. Vignale, and M. P. Das (Plenum, New York, 1998).
- ¹⁶G. Vignale, C. A. Ullrich, and S. Conti, *Phys. Rev. Lett.* **79**, 4878 (1997).
- ¹⁷G. Vignale, *Int. J. Mod. Phys. B* **15**, 1714 (2001).
- ¹⁸B. Champagne, D. H. Mosley, M. Vračko, and J. M. André, *Phys. Rev. A* **52**, 1039 (1995).
- ¹⁹M. Parac and S. Grimme, *J. Phys. Chem. A* **106**, 6844 (2002).
- ²⁰M. E. Casida, in *Recent Developments and Applications of Modern Density Functional Theory*, edited by J. M. Seminario (Elsevier, Amsterdam, 1996).
- ²¹S. J. A. van Gisbergen, J. G. Snijders, and E. J. Baerends, *Comput. Phys. Commun.* **118**, 119 (1999).
- ²²O. L. Brill and B. Goodman, *Am. J. Phys.* **35**, 832 (1967).
- ²³G. Breit, *Phys. Rev.* **39**, 616 (1932).
- ²⁴G. Breit, *Phys. Rev.* **34**, 553 (1929).
- ²⁵P. Nozières and D. Pines, *The Theory of Quantum Liquids* (Perseus, Cambridge, 1999), Chap. 4.7.
- ²⁶Z. X. Qian and G. Vignale, *Phys. Rev. B* **68**, 195113 (2003).
- ²⁷Z. Qian, A. Constantinescu, and G. Vignale, *Phys. Rev. Lett.* **90**, 066402 (2003).
- ²⁸C. A. Ullrich and G. Vignale, *Phys. Rev. B* **65**, 245102 (2002).
- ²⁹ADF2003.01, SCM, Theoretical Chemistry, Vrije Universiteit, Amsterdam, The Netherlands, <http://www.scm.com>, E. J. Baerends, J. A. Autschbach, A. Bérces *et al.*; the version we used in this article was modified by M. van Faassen.
- ³⁰E. J. Baerends, D. E. Ellis, and P. Ros, *Chem. Phys.* **2**, 41 (1973).
- ³¹L. Versluis and T. Ziegler, *J. Chem. Phys.* **88**, 322 (1988).
- ³²G. te Velde and E. J. Baerends, *J. Comput. Phys.* **99**, 84 (1992).
- ³³S. J. A. van Gisbergen, J. G. Snijders, and E. J. Baerends, *J. Chem. Phys.* **103**, 9347 (1995).
- ³⁴C. F. Guerra, J. G. Snijders, G. te Velde, and E. J. Baerends, *Theor. Chim. Acta* **99**, 391 (1998).
- ³⁵A. D. Becke, *Phys. Rev. A* **38**, 3098 (1988).
- ³⁶J. P. Perdew, *Phys. Rev. B* **33**, 8822 (1986).
- ³⁷S. H. Vosko, L. Wilk, and M. Nusair, *Can. J. Phys.* **58**, 1200 (1980).
- ³⁸K. E. Johnson, D. B. Johnston, and S. Lipsky, *J. Chem. Phys.* **70**, 3844 (1979).
- ³⁹R. Lindh and B. O. Roos, *Int. J. Quantum Chem.* **35**, 813 (1989).
- ⁴⁰C. Petrongolo, R. J. Buenker, and S. D. Peyerimhoff, *J. Chem. Phys.* **76**, 3655 (1982).
- ⁴¹J. D. Watts, S. R. Gwaltney, and R. J. Bartlett, *J. Chem. Phys.* **105**, 6979 (1996).
- ⁴²M. P. Pérez-Casany, I. Nebot-Gil, J. Sánchez-Marín, and O. Castell, *Chem. Phys. Lett.* **295**, 181 (1998).
- ⁴³E. R. Davidson and A. A. Jarzęcki, *Chem. Phys. Lett.* **285**, 155 (1998).
- ⁴⁴J. B. Platt, *J. Chem. Phys.* **17**, 484 (1949).
- ⁴⁵H. B. Klevens and J. B. Platt, *J. Chem. Phys.* **17**, 470 (1949).
- ⁴⁶R. P. Steiner and J. Michl, *J. Am. Chem. Soc.* **100**, 6861 (1978).
- ⁴⁷J. Wolf and G. Hohlneicher, *Chem. Phys.* **181**, 185 (1994).
- ⁴⁸Y. Kawashima, T. Hashimoto, H. Nakano, and K. Hirao, *Theor. Chim. Acta* **102**, 49 (1999).
- ⁴⁹P. Ilich, *Can. J. Spectrosc.* **32**, 19 (1987).
- ⁵⁰L. Serrano-Andrés and B. O. Roos, *J. Am. Chem. Soc.* **118**, 185 (1996).
- ⁵¹S. J. A. van Gisbergen, A. Rosa, G. Ricciardi, and E. J. Baerends, *J. Chem. Phys.* **111**, 2499 (1999).
- ⁵²R. van Leeuwen and E. J. Baerends, *Phys. Rev. A* **49**, 2421 (1994).
- ⁵³L. Edwards and D. H. Dolphin, *J. Mol. Spectrosc.* **38**, 16 (1971).
- ⁵⁴M. Klessinger and W. Lüttke, *Chem. Ber.* **99**, 2136 (1966).
- ⁵⁵L. Serrano-Andrés and B. O. Roos, *Chem.-Eur. J.* **3**, 717 (1997).
- ⁵⁶K. D. D'Amico, C. Manos, and R. L. Christensen, *J. Am. Chem. Soc.* **102**, 1777 (1980).
- ⁵⁷K. Nakayama, H. Nakano, and K. Hirao, *Int. J. Quantum Chem.* **66**, 157 (1998).
- ⁵⁸C. P. Hsu, S. Hirata, and M. Head-Gordon, *J. Phys. Chem. A* **105**, 451 (2001).
- ⁵⁹J. Pitarch-Ruiz, J. Sanchez-Marín, A. Sanchez De Meras, and D. Maynau, *Mol. Phys.* **101**, 483 (2003).
- ⁶⁰K. K. Innes, I. G. Ross, and W. R. Moomaw, *J. Mol. Spectrosc.* **132**, 492 (1988).
- ⁶¹J. G. G. Simon and A. Schweig, *Chem. Phys. Lett.* **200**, 631 (1992).
- ⁶²N. Ohmori, T. Suzuki, and M. Ito, *J. Phys. Chem.* **92**, 1086 (1988).
- ⁶³V. Molina and M. Merchán, *J. Phys. Chem. A* **105**, 3745 (2001).
- ⁶⁴M. Hanrath and S. D. Peyerimhoff, *Chem. Phys. Lett.* **337**, 368 (2001).
- ⁶⁵M. E. Boyle, B. E. Williamson, and P. N. Schatz, *Chem. Phys. Lett.* **125**, 349 (1986).
- ⁶⁶Y. S. Sohn, N. Hendrickson, and H. B. Gray, *J. Am. Chem. Soc.* **93**, 3603 (1971).
- ⁶⁷N. A. Beach and H. B. Gray, *J. Am. Chem. Soc.* **90**, 5713 (1968).
- ⁶⁸M. B. Robin, *Higher Excited States of Polyatomic Molecules* (Academic, New York, 1985).
- ⁶⁹M. Bavia, F. Bertinelli, C. Taliani, and C. Zauli, *Mol. Phys.* **31**, 479 (1976).
- ⁷⁰V. Huber, K. R. Asmis, A. C. Sergenton, and M. Allan, *J. Phys. Chem. A* **102**, 3524 (1998).
- ⁷¹M. Grüning, O. V. Gritsenko, S. J. A. v. Gisbergen, and E. J. Baerends, *J. Chem. Phys.* **114**, 652 (2001).
- ⁷²J. F. Dobson, *Phys. Rev. Lett.* **73**, 2244 (1994).
- ⁷³G. Vignale, *Phys. Rev. Lett.* **74**, 3233 (1995).
- ⁷⁴C. A. Ullrich and K. Burke (unpublished).
- ⁷⁵U. Nagashima, T. Takada, and K. Ohno, *J. Chem. Phys.* **85**, 4524 (1986).
- ⁷⁶B. F. Kim and J. Bohandy, *J. Mol. Spectrosc.* **73**, 332 (1978).
- ⁷⁷L. Serrano-Andrés, M. Merchán, M. Rubio, and B. O. Roos, *Chem. Phys. Lett.* **295**, 195 (1998).
- ⁷⁸K. N. Walzl, C. F. Koerting, and A. Kuppermann, *J. Chem. Phys.* **87**, 3796 (1987).
- ⁷⁹M. P. Fülischer, K. Andersson, and B. O. Roos, *J. Phys. Chem.* **96**, 9204 (1992).
- ⁸⁰C. R. C. Wang, S. Pollack, and M. M. Kappes, *Chem. Phys. Lett.* **166**, 26 (1990).
- ⁸¹V. Bonacic-Koutecký, P. Fantucci, and J. Koutecký, *Chem. Phys. Lett.* **166**, 32 (1990).
- ⁸²K. Pierloot, E. Tsokos, and L. G. Vanquickenborne, *J. Phys. Chem.* **100**, 16545 (1996).
- ⁸³O. Christiansen, J. Gauss, J. F. Stanton, and P. Jørgensen, *J. Chem. Phys.* **111**, 525 (1999).
- ⁸⁴S. Bashkin and J. A. Stoner, Jr., *Atomic Energy Levels and Grottrian Diagrams I* (North-Holland, Amsterdam, 1975).

The Journal of Chemical Physics is copyrighted by the American Institute of Physics (AIP). Redistribution of journal material is subject to the AIP online journal license and/or AIP copyright. For more information, see <http://ojps.aip.org/jcpo/jcpcr/jsp>
Copyright of Journal of Chemical Physics is the property of American Institute of Physics and its content may not be copied or emailed to multiple sites or posted to a listserv without the copyright holder's express written permission. However, users may print, download, or email articles for individual use.